ISSN 0036-0236, Russian Journal of Inorganic Chemistry, 2019, Vol. 64, No. 5, pp. 605–614. © Pleiades Publishing, Ltd., 2019.
Russian Text © The Author(s), 2019, published in Zhurnal Neorganicheskoi Khimii, 2019, Vol. 64, No. 5, pp. 490–499.

COORDINATION COMPOUNDS

Formation Reaction, Spectroscopy, and Photoelectrochemistry of the Donor–Acceptor Complex (5,10,15,20-Tetraphenyl-21,23H-porphinato)cobalt(II) with Pyridyl-Substituted Fullero[60]pyrrolidine

N. G. Bichan[a, *], E. N. Ovchenkova[a], V. A. Mozgova[a, b], N. O. Kudryakova[a], and T. N. Lomova[a]

[a] *Krestov Institute of Solution Chemistry, Russian Academy of Sciences, Ivanovo, 153045 Russia*

[b] *Ivanovo State University of Chemistry and Technology, Ivanovo, 153000 Russia*

**e-mail: bng@isc-ras.ru*

Received September 24, 2018; revised October 11, 2018; accepted October 15, 2018

Abstract—Kinetic and thermodynamic parameters of the donor–acceptor self-organization in the system (5,10,15,20-tetraphenyl-21H,23H-porphyrinato)cobalt(II) (CoTPP)–1-methyl-2-(pyridin-4'-yl)-3,4-fullero[60]pyrrolidine (PyC_{60})–toluene yielding the 1 : 2 complex $(PyC_{60})_2CoTPP$ are presented. The chemical structure of the supramolecular triad was elucidated by UV-vis, IR, and (^1H, ^{13}C) NMR spectroscopy. The photoelectrochemical characteristics of the $Ti|TiO_2$ electrode modified by the triad and its precursors were determined and the redox behavior of the latter was studied by cyclic voltammetry in dichloromethane.

Keywords: cobalt(II) porphyrin, fullero[60]pyrrolidine, donor–acceptor triad, kinetics and thermodynamics of formation, photoactivity

DOI: 10.1134/S0036023619050024

INTRODUCTION

Fullerenes are unique items possessing many advantages as functional materials for engineering and at the same time little studied objects for science. Fullerenes are known to be used as an anodic material to enhance battery capacities [1–3]. The use of fullerenes in organic photovoltaic cells with dry processing or non-halogenated solvent processing made it possible to obtain environmentally friendly and inexpensive photocells [4, 5]. Fullerenes are applicable in biomedical areas as powerful antioxidants that quickly react with free radicals [6] and as candidates for photodynamic therapy forming oxygen complexes under exposure to the visible light [7, 8]. Special attention has been paid to fullerene-modified composites in photovoltaics and optical devices [9, 10].

The ability of fullerenes to induce the rapid separation of opposite charges makes them promising components of photoactive supramolecular systems [11]. Porphyrins and their complexes have recently been widely used as the donor platform for such systems [12–19], because they are chromophores with high extinction coefficients, have electron-donating and electron-drawing properties, and are capable of forming π-type semiconductor layers [20, 21]. For example, the cobalt(II) complex with 5,10,15,20-tetraphenyl-21H,23H-porphyrin (CoTPP) has been studied during more than one decade [22, 23], but it yet remains topical today [24–27]. Multicomponent ionic complexes containing CoTPP and fullerenes (C_{60}, $C_{60}(CN)_2$, or C_{70}) were prepared [27, 28]. As probed by EPR and magnetic measurements, these complexes are diamagnetic and have electric conductivity of 2×10^{-3}–4×10^{-6} S/cm at room temperature. A rise in temperature above 320 K was shown to induce the dissociation of ionic complexes and to restore the paramagnetism of CoTPP [27]. Neutral CoTPP complexes with C_{60}, $C_{60}(CN)_2$, and C_{70} were also prepared [29]; they are insulators and manifest a paramagnetic behavior as opposed to ionic complexes.

The fluorescence quenching effect triggered an idea to use the donor–acceptor CoTPP complex with dansylpiperazine for NH_3 detection in nonpolar media [30]. A nanocomposite based on CoTPP and reduced graphene oxide manifests a high electrocatalytic activity for the oxidation and the reduction of H_2O_2 [31]. The highly stable noncovalent composite CoTPP–RGO (where RGO is reduced graphene oxide) [32] showed a more rapid electron transfer and a stronger electrocatalysis than CoTPP, RGO, or mixtures of the two which can make this composite a candidate material for design of sensors or bioelectrochemical devices.

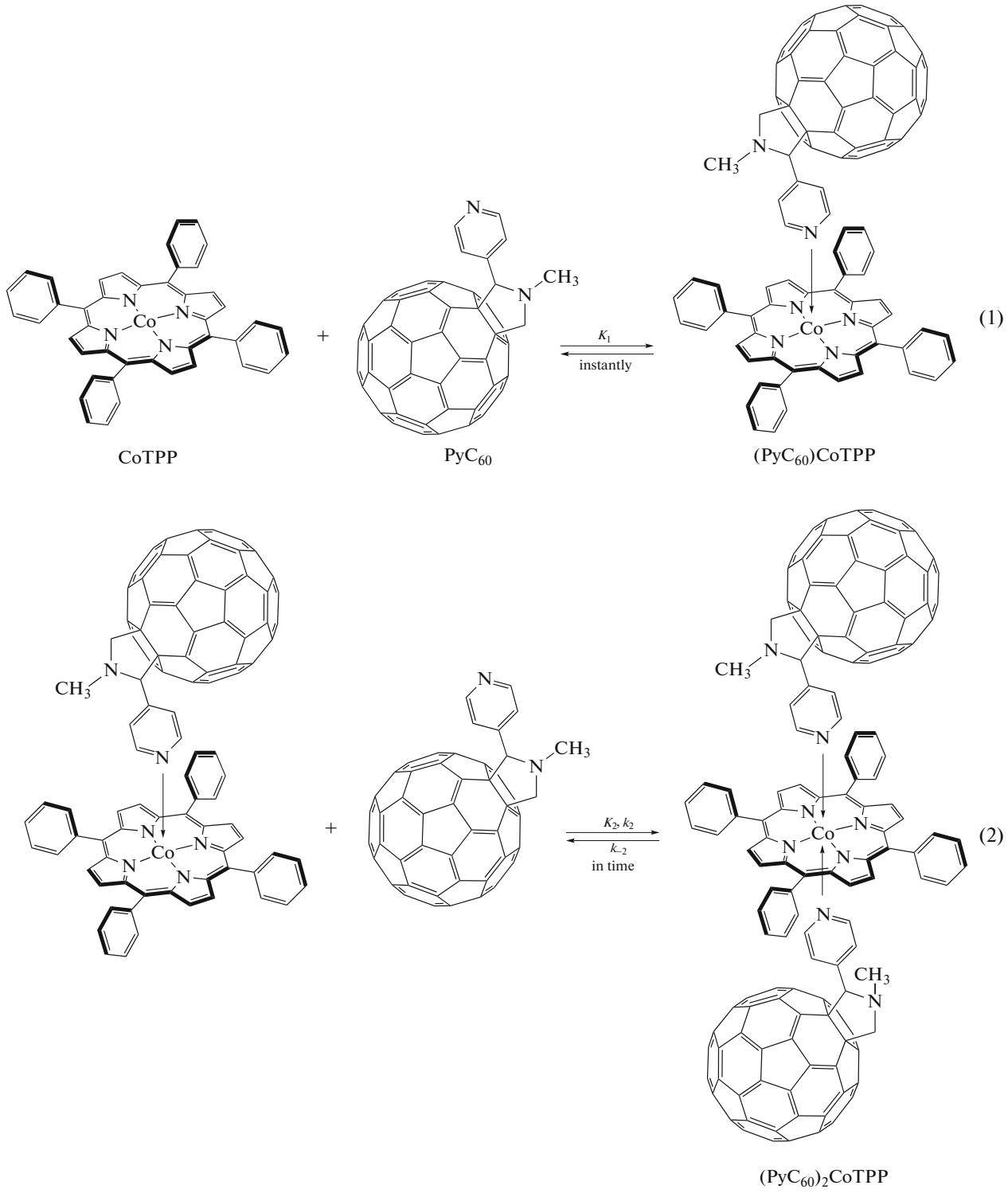

Fig. 1. Scheme of the formation of donor–acceptor porphyrin-fullerene complexes of CoTPP with PyC_{60}.

In order to further development the systems with predictable stability for photoelectrochemical cells, we used the reaction of the donor–acceptor CoTPP self-assembly with 1-methyl-2-(pyridin-4'-yl)-3,4-fullero[60]pyrrolidine (PyC_{60}) (Fig. 1) in this paper.

EXPERIMENTAL

(5,10,15,20-Tetraphenyl-21H,23H-porphinato)cobalt (II) (CoTPP) was prepared by the reaction of 5,10,15,20-tetraphenyl-21H,23H-porphine (H_2TPP) (50 mg, 0.081 mmol) with $Co(AcO)_2 \cdot 4H_2O$ (101 mg, 0.41 mmol)

in boiling dimethylformamide (DMF) for 10 min. When the reaction was over (as judged from the disappearance of H_2TPP bands and the end of evolution of the electronic absorption spectrum (UV-vis spectrum) of a reaction mixture sample in chloroform) the contents of the reaction flask were cooled and the products were extracted into chloroform after dilution with water. The solution in $CHCl_3$ was repeatedly washed with distilled water to remove DMF. The $CHCl_3$ was partially distilled off; the residual solution was purified by chromatography on an Al_2O_3-packed column (grade II activity according to Brockman) using chloroform. CoTPP yield: 87%. UV-vis spectrum in toluene (λ_{max} nm, (logε)): 413 (5.35), 529 (4.38). IR spectrum in KBr (ν, cm^{-1}): 415, 467, 527, 557, 567, 621, 650, 671, 700, 716, 751, 797, 835, 846, 900, 923, 997, 1005, 1020, 1071, 1155, 1178, 1205, 1236, 1309, 1350, 1441, 1492, 1540, 1576, 1599, 2852, 2922, 3025, 3052. ^{1}H NMR in $CDCl_3$ (δ, ppm): 9.83 (m, $12H_{m,p}$), 13.16 (br. s, $8H_o$),15.94 (br. s, $8H_\beta$). ^{13}C NMR in $CDCl_3$ (δ, ppm): 157.59, 141.79, 131.38, 130.92, 99.61. MS (MALDI-TOF) (*m/z*): 671.25 $[M]^+$.

1-Methyl-2-(pyridin-4'-yl)-3,4-fullero[60]pyrrolidine (PyC_{60}) was prepared by the described in [33] procedure modified to optimize the synthesis as to reagents, reaction time, and purification [34], namely, by the reacton of C_{60} with pyridin-4-carboxaldehyde and N-methylglycine in toluene for 2 h at the boiling temperature of the mixture. Yield: 52%. The PyC_{60} was purified by chromatography on an Al_2O_3-packed column (grade II activity according to Brockman) (toluene–ethyl acetate 20 : 1). UV-vis spectrum in toluene (λ_{max} nm, (logε)): 312, 328, 433 (3.56). IR spectrum in KBr (ν, cm^{-1}): 404, 431, 448, 479, 504, 527, 553, 574, 598, 635, 664, 707, 737, 767, 785, 824, 840, 910, 940, 989, 1034, 1067, 1083, 1109,1123, 1179, 1215, 1246, 1268, 1314, 1334, 1409, 1430, 1463, 1561, 1595, 1736, 2783, 2845, 2920, 2948. ^{1}H NMR in $CDCl_3$ (δ, ppm (*J*, Hz)): 2.83 (s, 3H), 4.31 (d, $J = 9.77$, 1H), 4.96 (s, 1H), 5.02 (d, $J = 9.77$, 1H), 7.82 (m, 2H), 8.71 (d, $J = 5.49$, 2H). ^{13}C NMR in $CDCl_3$ (δ, ppm): 155.89, 153.74, 152.54, 152.02, 149.52, 147.63, 146.60, 146.51, 146.25, 145.92, 145.74, 145.65, 145.52, 144.98, 144.79, 144.69, 144.58, 143.45, 143.30, 143.03, 142.91, 142.84, 142.46, 142.33, 142.09, 142.13, 142.05, 141.97, 141.85, 140.53, 140.23, 139.85, 137.38, 136.53, 136.36, 135.80, 129.26, 128.46, 124.72, 82.53, 70.26, 69.39, 40.23. MS (MALDI-TOF) (*m/z*, relative intensity, %): 853 (99) $[M - H]^+$, 854 (76) $[M]^+$.

(5,10,15,20-Tetraphenyl-21H,23H-porphinato)*bis*-(1-methyl-2-(pyridin-4'-yl)-3,4-fullero[60]pyrrolidine)cobalt(II) ($(PyC_{60})_2$CoTPP) was prepared by an original procedure by the reaction between CoTPP and PyC_{60} (in the molar ratio 1 : 5) in toluene at 298 K for 30 min. The synthesis was ended when the UV-vis spectrum of the reaction mixture ceased to change. The solid $(PyC_{60})_2$CoTPP sample mixed with an excess of PyC_{60} was obtained by distilling off toluene. The spectral characteristics of the individual triad $(PyC_{60})_2$CoTPP were gained by quantitatively subtracting the PyC_{60} spectra. UV-vis spectrum in toluene (λ_{max}, nm): 434 (**I**), 555 (**II**) with the intensity ratio **I** > **II**. IR spectrum in KBr (ν, cm^{-1}): 413, 428, 464, 479, 486, 505, 527, 541, 553, 562, 575, 583, 598, 607, 621, 636, 665, 701, 715, 725, 737, 752, 767, 797, 825, 832, 840, 909, 921, 939, 995, 1004, 1019, 1038, 1072, 1108, 1123, 1142, 1153, 1162, 1177, 1205, 1231, 1245, 1267, 1281, 1313, 1334, 1351, 1371, 1410, 1421, 1429, 1440, 1463, 1492, 1542, 1561, 1575, 1598, 2782, 2847, 2920, 2948, 3021, 3052. ^{1}H NMR in $CDCl_3$ (δ, ppm): 2.26 (s, $H_{CH_3-PyC_{60}}$), 3.40 (br. s, $H_{PyC_{60}}$), 4.12 (br. s, $H_{PyC_{60}}$), 7.67 (m, $H_{m-PyC_{60}}$), 8.56 (m, $H_{m,p}$), 9.08 (s, $H_{o-PyC_{60}}$), 9.88 (br. s, H_o), 13.50 (br. s, H_β). ^{13}C NMR in $CDCl_3$ (δ, ppm): 153.68, 152.64, 151.01, 148.11, 144.99, 144.38, 143.54, 142.71, 142.30, 139.30, 139.09, 138.56, 130.17, 129.96, 129.66, 128.86, 128.21, 127.32, 126.41, 125.93, 71.33, 66.96, 40.17, 30.32, 22.08, 20.33.

Toluene (EKOS type) was dried by potassium hydroxide and distilled before use (T_b= 110.6°C). The water content according to Fisher did not exceed 0.01%.

The kinetics of the reversible reaction of CoTPP with PyC_{60} in toluene was studied spectrophotometrically at 298 K at PyC_{60} concentrations in the range from 3.97×10^{-5} to 8.93×10^{-5} mol/L by the excessive concentration method. Solutions of CoTPP and PyC_{60} in freshly distilled toluene were prepared immediately before use to avoid peroxide formation in the solvent. Optical density measurements for a set of solutions of a constant CoTPP concentration of 6.13×10^{-6} mol/L, and a variable concentration of the substituted fullerene were carried out on the working wavelength 413 nm immediately after the reagents were combined and then over time. The UV-vis spectra of the reacting system were recorded with the spectrum of PyC_{60} in the same concentration as in the working solution used as the baseline. The solutions were thermostated at (298 ± 0.1) K in closed quartz cuvette in a special cell of the spectrophotometer. Reaction rate constants were calculated by Eq. (3).

$$k_{eff} = (1/\tau)\ln\left((A_0 - A_\infty)/(A_\tau - A_\infty)\right). \quad (3)$$

Here A_o, A_τ, and A_∞ are the optical densities of the reaction mixture at $\lambda = 413$ nm in the moments of time 0 and τ, and upon the end of the reaction.

The equilibrium of the CoTPP reaction with PyC_{60} in toluene was studied at 298 K and $c_{CoTPP} = 6.13 \times 10^{-6}$ mol/L at PyC_{60} concentrations in the range from 4.96×10^{-6} to 8.93×10^{-5} mol/L; the spectrophotometric titration was recorded by the molar ratios method taking into account the time to establish equilibria [35]. Equilibrium constants (*K*) were determined by Eq. (4)

for a three-component (CoTPP, PyC_{60}, and $(PyC_{60})_2CoTPP$) equilibrium system with two colored compounds by the least squares in Microsoft Excel:

$$K = \frac{(A_i - A_0)/(A_\infty - A_0)}{1 - (A_i - A_0)/(A_\infty - A_0)} \times \frac{1}{(c^0_{PyC_{60}} - c^0_{CoTPP}(A_i - A_0)/(A_\infty - A_0))}, \quad (4)$$

where $c^0_{PyC_{60}}$ and c^0_{CoTPP} are, respectively, the initial PyC_{60} and CoTPP concentration in toluene; A_0, A_i, and A_∞ are, respectively, optical densities of CoTPP, the equilibrium mixture, and reaction product at λ = 413 nm. The relative error in K did not exceed 25%. The reaction stoichiometry was determined as the tangent of the line $\log(A_i - A_0)/(A_\infty - A_i)$–$f(\log c_{PyC_{60}}$ [mol/L]) ($\log I$ – $f(\log c_{PyC_{60}}$ [mol/L])).

UV-vis, IR, NMR, and mass spectra were recorded on an Agilent 8453 spectrometer, VERTEX 80v, Bruker Avance III-500 spectrometers, and a Shimadzu Confidence mass spectrometer, respectively.

The photoelectrochemical properties of the titanium anode with a natural oxide film (NOF) modified by CoTPP, PyC_{60}, and $(PyC_{60})_2CoTPP$, were studied in a quartz cell (light transmission: 92–95%) at (298 ± 2) K. A test sample was exposed to a monochromated UV light (365 nm) with the intensity 1.5 mW/cm^2 using a MiniMAX UV-5A/F lamp. The measured parameters were photocurrent density (j_{ph}) and the incident photon-to-current conversion efficiency (IPCE, the "monochromatic version" of the external quantum yield). The photocurrent was measured in the short-circuited electrochemical cell Ti|film $CoTPP/PyC_{60}/(PyC_{60})_2CoTPP$|0.5 mol/L Na_2SO_4|Pt, which was equipped with a V7-77 voltmeter. The distance between the electrodes was 2 mm. The numerical values of IPCE were calculated by Eq. (5).

$$IPCE = \frac{1240 j_{sc}}{\lambda P_{in}}. \quad (5)$$

Here j_{sc} is the short circuit current density, mA/cm^2; λ is the monochromatic light wavelength, nm; and P_{in} is the specific power of the incident light, mW/cm^2.

Electrochemical measurements were carried out at room temperature (298 K) under anaerobic conditions in a three-electrode cell using a PI 50-Pro-3 pulse potentiostat with software PS Pack 2. Voltammetric curves were recorded at the potential sweep rate 100 mV/s. The working electrode and counterelectrode used were a platinum electrode and platinum wire, respectively. The reference electrode was a saturated calomel electrode. The electrochemical studies of CoTPP, PyC_{60}, and $(PyC_{60})_2CoTPP$ were carried out in their freshly prepared solutions in dichloromethane with addition of an ancillary electrolyte (0.1 mol/L (n-Bu)$_4$NClO$_4$) under an argon flow.

RESULTS AND DISCUSSION

The data of spectral methods reliably characterize the prepared CoTPP as a porphyrin complex of divalent cobalt. A change in the degree of oxidation of cobalt in the porphyrin molecule or addition of axial ligands induces great changes in the UV-vis spectra [34, 36, 37], so this approach is suitable for studying their properties.

The UV-vis spectrum of CoTPP in toluene features the Soret band ($1a_{1g} \rightarrow 2e_u$) at 413 nm and the Q band ($1a_{1g} \rightarrow 1e_u$) at 529 nm [38]. An analysis of the UV-vis spectrum dynamics (Figs. 2, 3) allowed to detect two equilibria in the course of the CoTPP reaction with PyC_{60}. The first equilibrium is acquired immediately as the reagent solutions are combined and the second is acquired over time; that is, the process is two-step in the temporary field (unlike classic two-step reactions in the concentration field). The processing of titration data, the identification of the reaction product, the nonoccurrence of association-type PyC_{60} conversions [34] and aggregation under the spectrophotometric experimental conditions proved the occurrence of consecutive two-step reactions of the coordination of two PyC_{60} molecules to the central atom in CoTPP (Fig. 1).

The spectral pattern of the CoTPP reaction with PyC_{60} in toluene when $\tau = 0$ (the first step) is shown in Fig. 2. After equilibrium is attained at the first step, for all reaction mixtures the subsequent slow reaction in the system CoTPP–PyC_{60} is accompanied by a gradual reduction in absorption at 413 and 529 nm and the appearance of new bands at 434 and 555 nm, proving the formation of a hexacoordinate cobalt complex [34, 39]. The reaction is reversible: equilibrium is attained in 30 min or less depending on the fullerene concentration (Fig. 3). The first and second reaction steps each involve one PyC_{60} molecule ($\tan\alpha = 0.83$ (Fig. 2c) and 1.19 (Fig. 3c), respectively). The numerical values of equilibrium constants are $K_1 = (5.43 \pm 1.21) \times 10^4$ L/mol ($\log K_1 = 4.73$) and $K_2 = (8.69 \pm 1.39) \times 10^4$ L/mol ($\log K_2 = 4.94$). The stability (formation) constant of $(PyC_{60})_2CoTPP$ written as $\beta = K_1K_2$ is $(4.69 \pm 1.23) \times 10^9$ L^2/mol^2 ($\log\beta = 9.67$).

In the course of the kinetic study of the slow forward reaction of the second equilibrium step (Fig. 4, Eq. (2)), the reaction was determined to have a first order with respect to $(PyC_{60})CoTPP$ and thereby to CoTPP (quasi-equilibrium). Effective rate constants (k_{2eff}) appear in Table 1.

Linear plots $\log k_{2eff}$ [s^{-1}]–$f(\log c_{PyC_{60}}$ [mol/L]) with a near-unity slope ($\tan\alpha = 0.80$) (Fig. 4b) indicate a first order of the reaction with respect to PyC_{60}. The numerical value of the rate constant k_2 is 9.57 ± 0.15 L/(mol s). The rate constant k_{-2} is 1.1×10^{-4} s^{-1} (9.57 L/(mol s)/ 8.69×10^4 L/mol). The ratio of the rate constants of the forward and back reactions (k_2 and k_-

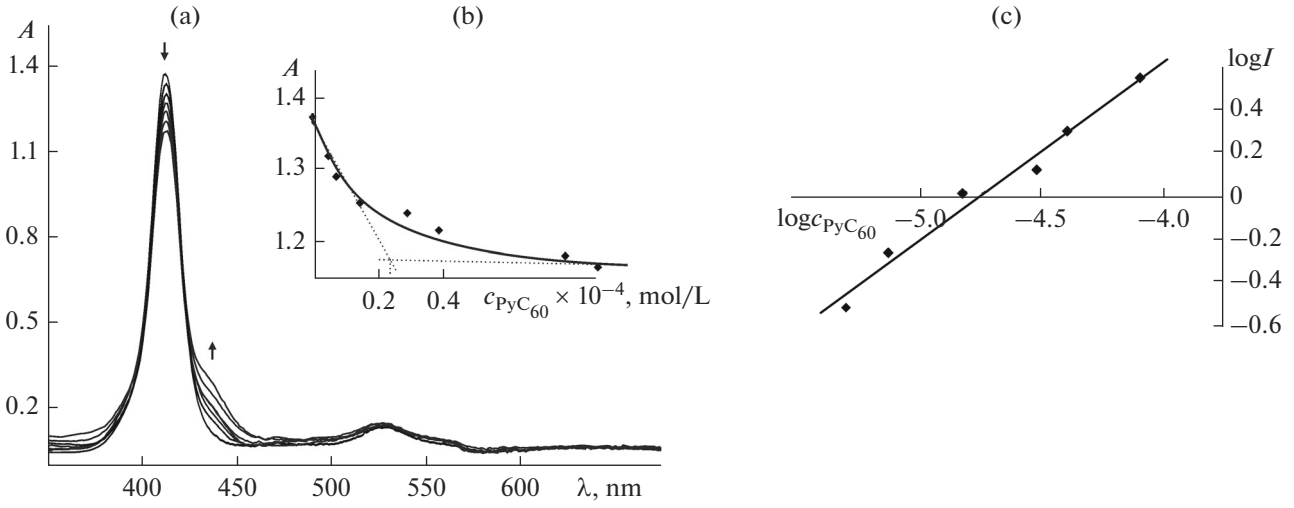

Fig. 2. (a) Evolution of the CoTPP UV-vis spectrum in toluene at 298 K with PyC_{60} addition (in toluene solution) in the range from 0 to 8.93×10^{-5} mol/L, (b) the respective spectrophotometric titration curve obtained at the working wavelength 413 nm, and (c) log$I$ *versus* log$c_{PyC_{60}}$ plot ($R^2 = 0.98$) for the reaction of CoTTP with PyC_{60} at 298 K and $\tau = 0$.

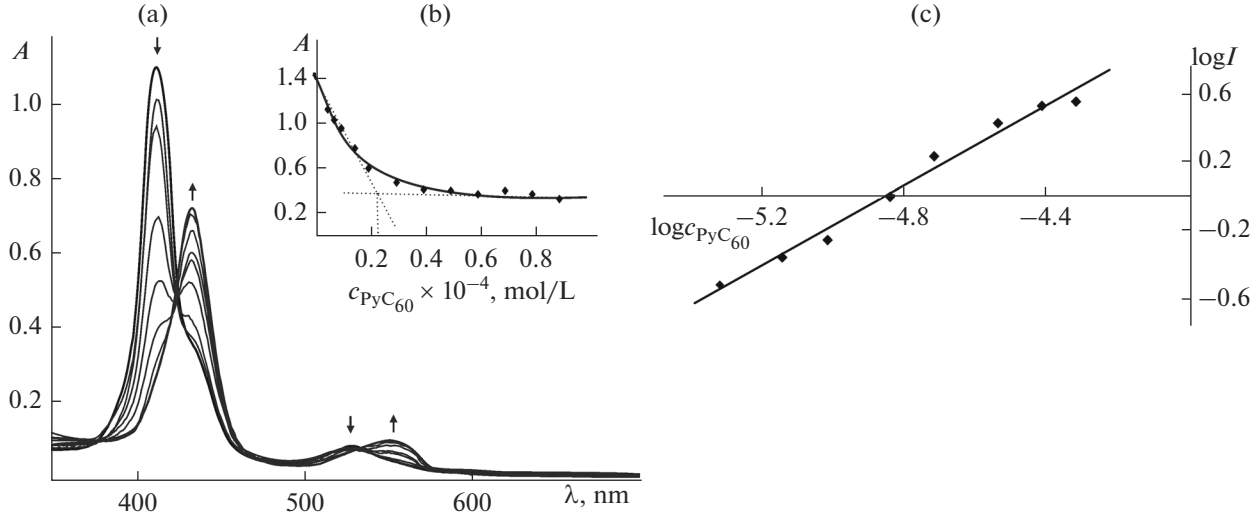

Fig. 3. (a) Evolution of the CoTPP UV-vis spectrum at 298 K with PyC_{60} addition (in toluene solution) in the range from 4.96×10^{-6} to 8.93×10^{-5} mol/L, (b) the respective spectrophotometric titration curve obtained at the working wavelength 413 nm, and (c) log$I$ *versus* log$c_{PyC_{60}}$ plot ($R^2 = 0.98$) for the reaction of CoTTP with PyC_{60} at 298 K and $\tau = \infty$.

$_2$) indicates the admissibility of neglecting the back reaction when studying the kinetics of the two-way process in the second step stage of the CoTPP reaction with PyC_{60}.

The IR spectrum of $(PyC_{60})_2$CoTPP (Fig. 5) features new signals (against the CoTPP spectrum) with the frequencies 2948, 2920, 2847, 2782, 1561, 1463, 1429, 1421, 1410, 1371, 1334, 1267, 1245, 1162, 1123, 1108, 939, 909, 825, 737, 725, 636, 607, 598, 575, 541, 527, 505, 479, and 428 cm^{-1}, corresponding to the vibrations of N-bonded PyC_{60}. The signals at 1429, 575, and 527 cm^{-1} correspond to the vibrations of the fullerene cage C_{60} [40] and they do not change their positions upon triad formation. The vibrational frequencies of the pyridine ring and pyrrolidine ring of fullerene increase by about 1–17 cm^{-1} against the vibrations in the initial PyC_{60} (see Experimental). The chemical modification of metal porphyrins by means of the axial bonding of ligands is known to change the skeletal vibrations of porphyrin molecules in the IR spectrum due to the shift of the metal from the macrocyclic plane [41]. In our case, the position and intensity of

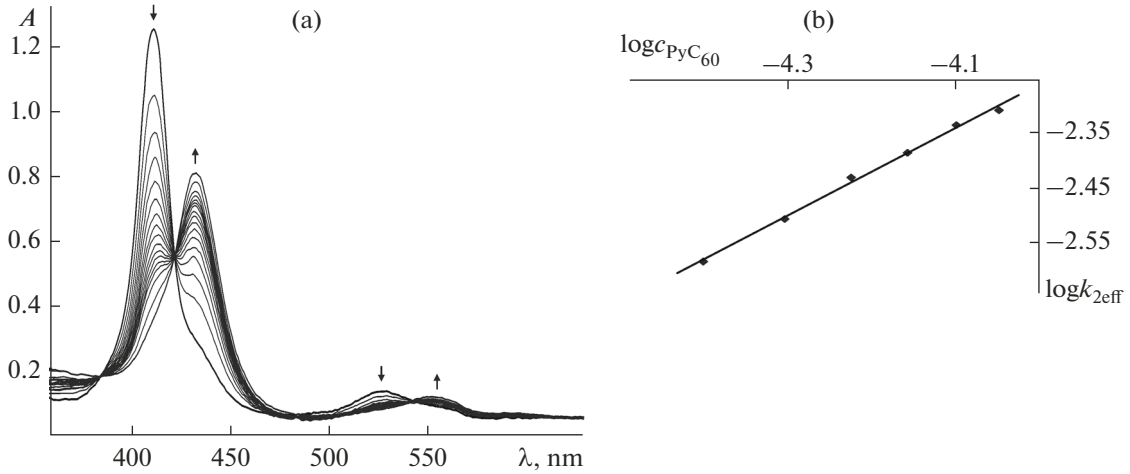

Fig. 4. (a) Evolution of the (PyC_{60})CoTPP electronic absorption spectrum in toluene at 298 K with PyC_{60} addition of 5.95×10^{-5} mol/L in toluene at 298 K for 30 min and (b) $\log k_{2eff}$ [s^{-1}]–$\log C_{PyC_{60}}$ plot [mol/L] ($R^2 = 0.99$).

vibrations of the CoTPP pyrrole rings remain almost unchanged in the $(PyC_{60})_2$CoTPP spectrum; therefore, the Co remains in the macrocyclic plane upon the coordination of two PyC_{60} molecules. This observation is supported by theoretical calculations [42].

The ^{1}H NMR spectrum of CoTPP points to the paramagnetism of the complex. Evidence for this comes from the low-field position and the broadening of β-proton signals at 15.94 ppm and the protons of phenyl substituents at 13.16 and 9.83 ppm (Fig. 6a). These signals in the $(PyC_{60})_2$CoTPP spectrum experience a strong upfield shift. The H_β signals experience a 2.44-ppm shift and appear at 13.50 ppm; H_o and $H_{m,p}$ signals of the phenyl substituents of CoTPP shift to 9.88 and 8.56 ppm, respectively (Fig. 6b). Such shifts of resonance signals of the $(PyC_{60})_2$CoTPP macrocycle proton may be explained by a weakening in the circular current effect of the porphyrin ring as a result of the formation of donor–acceptor bonds $Co - N_{PyC_{60}}$. The ^{13}C NMR spectrum of $(PyC_{60})_2$CoTPP also proves the formation of a donor–acceptor complex, in the spectrum of which the carbon signals of the substituted fullerene and porphyrin ring shift relative to the respective signals in the spectra its precursors (Fig. 7).

Table 1. Effective rate constants (k_{2eff}) of the (PyC_{60})CoTPP reaction with PyC_{60} in toluene at 298 K

$c_{PyC_{60}} \times 10^{-5}$, mol/L	$(k_{2eff} \pm \delta k_{2eff}) \times 10^3$, s^{-1}
3.97	2.61 ± 0.21
4.96	3.11 ± 0.09
5.95	3.72 ± 0.18
6.94	4.08 ± 0.32
7.93	4.59 ± 0.32
8.93	4.90 ± 0.31

Previously we studied the analogous reaction involving (5,10,15,20-(tetra-4-*tert*-butylphenyl)-21H,23H-porphinato)cobalt(II) (Co^{t}BPP) [34] and (2,3,7,8,12,18-hexamethyl,13,17-diethtyl,5-(2-pyridyl)porphinato)cobalt(II) (CoP) [42]. The formation constants of 1 : 2 complexes in these cases are, respectively, $(1.34 \pm 0.12) \times 10^{10}$ L^2/mol^2 ($\log\beta = 10.13$) and $(1.04 \pm 0.12) \times 10^{10}$ L^2/mol^2 ($\log\beta = 10.02$). We may state that the electron-donating substituents in the cobalt(II)porphyrin structure (*tert*-butyl groups in Co^{t}BPP and methyl/ethyl groups in CoP), as the absence of electron-drawing phenyls (in CoP), too, favor strengthening of $Co-N_{PyC_{60}}$ bonds in donor–acceptor complexes.

The photoactivity study of the titanium dioxide electrode modified by the donor–acceptor triad $(PyC_{60})_2$CoTPP (Table 2), showed that the photoelectrochemical characteristics (photocurrent density and IPCE) are independent of the solvent (CH_2Cl_2, $CHCl_3$, or toluene) from which modifier layers (films) were prepared. CoTPP, PyC_{60}, and $(PyC_{60})_2$CoTPP in toluene/dichloromethane and quartz supported films have identical UV-vis spectra. The photocurrent density and IPCE values of films were measured in the short-circuited electrochemical cell Ti|film|0.5 mol/L Na_2SO_4|Pt with the modified titanium electrode exposed to the light with λ = 365 nm. With electrodes modified by $(PyC_{60})_2$CoTPP and $(PyC_{60})_2$Co^{t}BPP [34], the photocurrent increased from the zero for the titanium electrode with a NOF to 77.53 and 85.80 μA/cm^2, respectively; these values exceed j_{ph} for individual components of donor–acceptor systems. The IPCE values for $(PyC_{60})_2$CotPP and $(PyC_{60})_2$CoTBPP,

reaching 40.22 and 42.18% at λ_{exc} = 365 nm, are also higher than for the individual components.

The films modified by (porphyrinato)cobalt(II) that contains peripheral electron-donating substituents have highest values of photocurrent density and IPCE. For example, IPCE (excited by the 365-nm light) for the donor–acceptor triad based on (2,3,7,8,12,18-hexamethyl,13,17-diethtyl,5-(2-pyridyl)porphinato)cobalt(II) and PyC_{60} is 69.16% [42] against 40.22% for $(PyC_{60})_2CoTPP$. The insertion of electron-donating *tert*-butyl groups into phenyl rings in Co′BPP results in an intermediate IPCE value (42.18%).

Figure 8a shows a cyclic voltammetric (CVA) curve for PyC_{60} in dichloromethane ($c_{PyC_{60}} = 4.03 \times 10^{-4}$ mol/L); this curve features three pairs of peaks typical of fulleropyrrolidines [43–45]. There are three peaks for PyC_{60} in the area of negative potentials due to fullerene reduction to yield a π-anion radical (–0.78 V), a dianion (–1.10 V), and a trianion (–1.62 V) and conjugated oxidation peaks (–1.55, –1.04, and –0.57 V). The CVA for CoTPP ($c = 1.03 \times 10^{-3}$ mol/L) coincides with the reported data [46]. There are three reversible peaks (CoTPP oxidation) and one irreversible peak (CoTPP reduction) in the area of positive and negative potentials. In order to observe the CVA of $(PyC_{60})_2CoTPP$, we took the precursors of the triad in the molar ratio corresponding to the equivalence point in spectrophotometric titration ($c_{CoTPP} = 8.56 \times 10^{-5}$ mol/L, $c_{PyC_{60}} = 5.13 \times 10^{-4}$ mol/L). The 100% transition of CoTPP to $(PyC_{60})_2CoTPP$ is accompanied by a positive shift of the redox potentials of fullerene (reduction peaks: –0.66, –0.7, and –1.08 V; oxidation peaks:–1.01, –0.61, and 0.02 V); this points to interaction between the π system of CoTPP (the donor) and the fullerene moiety PyC_{60} (acceptor) (Fig. 8b). The peaks of the porphyrin component do not appear in the CVA of the triad due to its low concentration (8.56×10^{-5} mol/L).

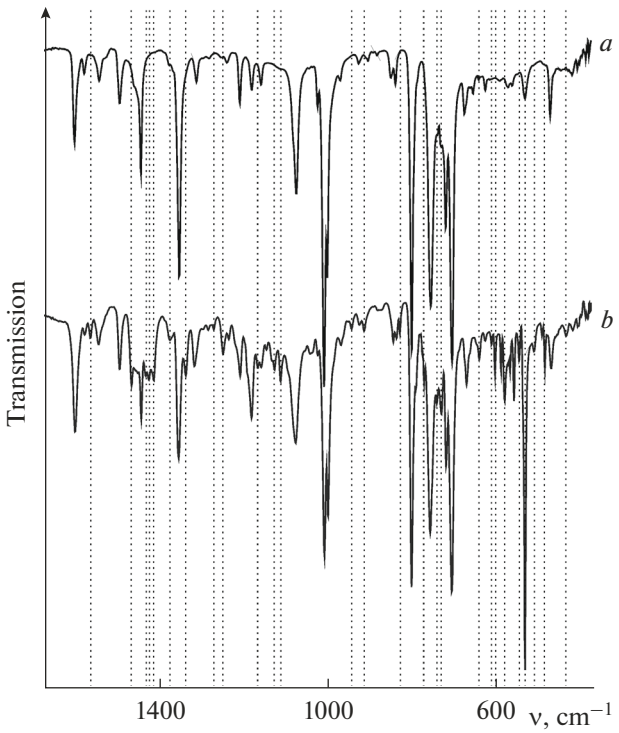

Fig. 5. IR spectra of (a) CoTPP and (b) donor–acceptor complex $(PyC_{60})_2CoTPP$ in KBr.

CONCLUSIONS

We have studied the donor–acceptor 1 : 2 complex formation reaction between (5,10,15,20-tetraphenyl)-21H,23H-porphinato)cobalt(II) and 1-methyl-2-(pyridin-4'-yl)-3,4-fullero[60]pyrrolidine by UV-vis spectroscopy, chemical kinetics, and thermodynamics. The chemical structure of the $(PyC_{60})_2CoTPP$ triad has been elucidated by spectral methods, namely, by UV-vis, IR, and (^1H, ^{13}C) NMR spectroscopy; the stability constants β has been found to be $(4.69 \pm 1.23) \times 10^9$ L^2/mol^2. The electrochemical (CVA) and photoelectrochemical (photocurrent density and IPCE) parameters have been obtained for the $(PyC_{60})_2CoTPP$ triad and its precursors. Using similar data for the tetra-4-*tert*-butyl-substituted analogue

Table 2. Photocurrent density and IPCE of the system Ti|film|0.5 mol/L Na_2SO_4|Pt

Titanium electrode with a natural oxide film (NOF)	j_{ph}^{avg}, μA/cm²	$IPCE^{365\ nm}$, %
NOF	0	0
CoTPP ($c_{CoTPP} = 3.5 \times 10^{-6}$ mol/L)	77.53	18.68
Co′BPP ($c_{Co'BPP} = 4.2 \times 10^{-6}$ mol/L) [34]	85.80	20.67
PyC_{60} ($c_{PyC_{60}} = 2.7 \times 10^{-5}$ mol/L)	78.95	19.02
$(PyC_{60})_2CoTPP$ ($c_{CoTPP} = 3.5 \times 10^{-6}$ mol/L, $c_{PyC_{60}} = 2.7 \times 10^{-5}$ mol/L)	166.91	40.22
$(PyC_{60})_2Co'BPP$ ($c_{Co'BPP} = 4.2 \times 10^{-6}$ mol/L, $c_{PyC_{60}} = 2.7 \times 10^{-5}$ mol/L) [34]	175.05	42.18

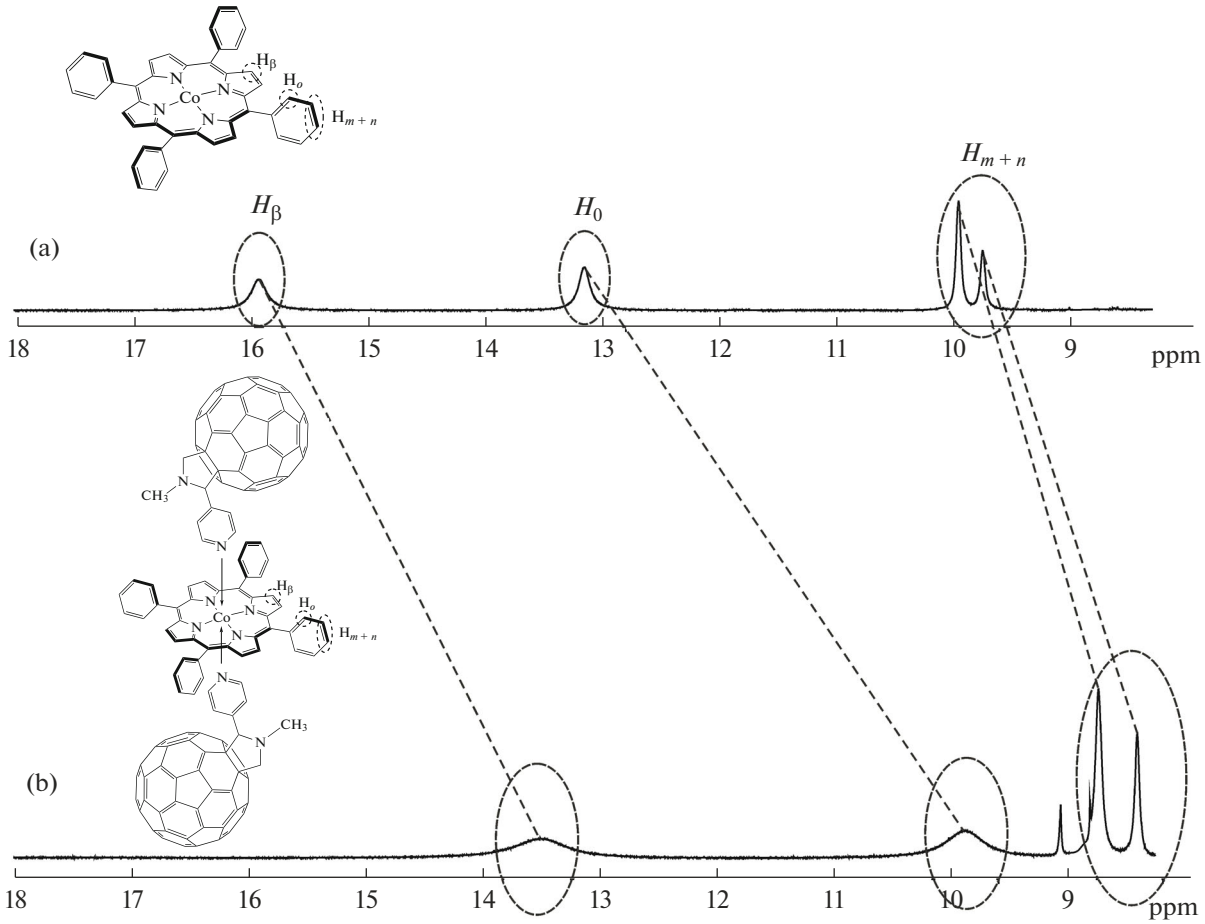

Fig. 6. ^{1}H NMR spectra of (a) CoTPP and (b) donor–acceptor complex $(PyC_{60})_2CoTPP$ in $CDCl_3$.

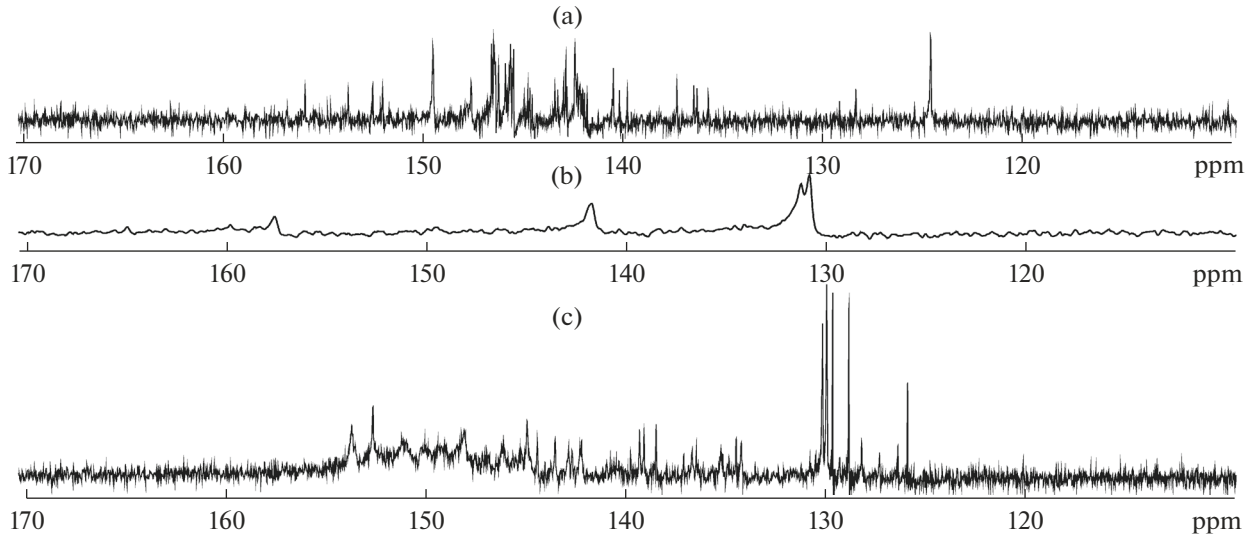

Fig. 7. ^{13}C NMR spectra of (a) PyC_{60}, (b) CoTPP, and (c) donor–acceptor complex $(PyC_{60})_2CoTPP$ in $CDCl_3$.

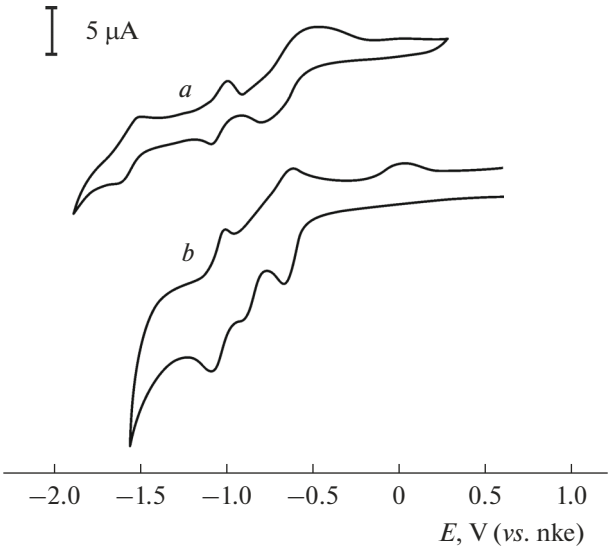

Fig. 8. Cyclic voltammetry curves of (*a*) PyC_{60} and (*b*) $(PyC_{60})_2CoTPP$ in dichloromethane. Potential sweep rate: 100 mV/s.

$(PyC_{60})_2Co^tBPP$ [34], a correlation was found among the stability, photoelectrochemical parameters, and molecular structure of donor–acceptor porphyrin fullerene complexes; this correlation can potentially be used in design of donor–acceptor systems for photoelectrochemical cells.

ACKNOWLEDGMENTS

This study was performed on the equipment of the Shared Facilities Center "Upper Volga Physicochemical Research Center" and was financially supported by the Russian Foundation for Basic Research and the Government of the Ivanovo oblast (nos. 18-43-370023 and 18-43-370022 (synthesis)).

REFERENCES

1. M. Li, Y.-J. Liu, J.-X. Zhao, et al., Appl. Surf. Sci. **355**, 1145 (2015). https://doi.org/10.1016/j.apsusc.2015.03.144
2. M. Moradi, Z. Bagheri, and A. Bodaghi, Physica E **89**, 148 (2017). https://doi.org/10.1016/j.physe.2017.02.018
3. L. Qiao, X. Sun, Z. Yang, et al., Carbon **54**, 29 (2013). https://doi.org/10.1016/j.carbon.2012.10.066
4. K. Tada, Sol. Energy Mater. Sol. Cells **130**, 331 (2014). https://doi.org/10.1016/j.solmat.2014.07.032
5. K. Tada, Appl. Phys. Express **7**, 051601 (2014). https://doi.org/10.7567/APEX.7.051601
6. N. V. Kalacheva, G. R. Tarasova, G. M. Fazleeva, et al., Bioorg. Med. Chem. Lett. **28**, 1097 (2018). https://doi.org/10.1016/j.bmcl.2018.02.009
7. Z. Chen, L. Ma, Y. Liu, et al., Theranostics **2**, 238 (2012). https://doi.org/10.7150/thno.3509
8. S. Goodarzi, T. Da Ros, J. Conde, et al., Mater. Today **20**, 460 (2017). https://doi.org/10.1016/j.mattod.2017.03.017
9. N. Yu. Borovkov and S. V. Blokhina, Colloids Surf., A: Physicochem. Eng. Aspects **377**, 393 (2011). https://doi.org/10.1016/j.colsurfa.2011.01.044
10. M. Baibarac, I. Baltog, M. Daescu, et al., J. Mol. Struct. **1125**, 340 (2016). https://doi.org/10.1016/j.molstruc.2016.07.001
11. B. Chandra and F. D'Souza, Coord. Chem. Rev. **322**, 104 (2016). https://doi.org/10.1016/j.ccr.2016.05.012
12. C. Solis, M. B. Ballatore, M. B. Suarez, et al., Electrochim. Acta **238**, 81 (2017). https://doi.org/10.1016/j.electacta.2017.04.015
13. L.-L. Li and E. W.-G. Diau, Chem. Soc. Rev. **42**, 291 (2013). https://doi.org/10.1039/C2CS35257E
14. T. Higashino and H. Imahori, J. Chem. Soc., Dalton Trans. **44**, 448 (2015). https://doi.org/10.1039/C4DT02756F
15. M. Urbani, M. Gratzel, M. K. Nazeeruddin, et al., Chem. Rev. **114**, 12330 (2014). https://doi.org/10.1021/cr5001964
16. H. Imahori, T. Umeyama, K. Kurotobi, et al., Chem. Commun. **48**, 4032 (2012). https://doi.org/10.1039/C2CC30621B
17. T. N. Lomova, E. V. Motorina, and M. V. Klyuev, *CRC Concise Encyclopedia of Nanotechnology*, Ed. by B. I. Kharisov, O. V. Kharissova, and U. Ortiz-Mendez (CRC Press, London, 2016).
18. E. V. Motorina, T. N. Lomova, and M. V. Klyuev, Mend. Commun. **28**, 426 (2018). https://doi.org/10.1016/j.mencom.2018.07.029
19. E. N. Ovchenkova, N. G. Bichan, N. O. Kudryakova, et al., Dyes Pigm. **153**, 225 (2018). https://doi.org/10.1016/j.dyepig.2018.02.023
20. J. M. Gottfried, Surf. Sci. Rep. **70**, 259 (2018). https://doi.org/10.1016/j.surfrep.2015.04.001
21. D. M. Lyons, J. Kesters, W. Maes, et al., Synth. Met. **178**, 56 (2013). https://doi.org/10.1016/j.synthmet.2013.06.013
22. S. Ciurli, S. Gambarotta, C. Floriani, et al., Angew. Chem., Int. Ed. Engl. **98**, 553 (1986).
23. S. Fukuzumi and J. Maruta, Inorg. Chim. Acta **226**, 145 (1994). https://doi.org/10.1016/0020-1693(94)04080-X
24. W. Choi, P. G. Ingole, H. Li, et al., J. Cleaner Prod **133**, 1008 (2016). https://doi.org/10.1016/j.jclepro.2016.06.031
25. L. P. H. Saravia, S. Anandhakumar, A. L. A. Parussulo, et al., J. Electroanal. Chem. **775**, 72 (2016). https://doi.org/10.1016/j.jelechem.2016.05.026
26. H. Li, W. Choi, P. G. Ingole, et al., Fuel **185**, 133 (2016). https://doi.org/10.1016/j.fuel.2016.07.097

27. D. V. Konarev, S. S. Khasanov, A. Otsuka, et al., J. Chem. Soc., Dalton Trans., No. 32, 6416 (2009). https://doi.org/10.1039/B904293H
28. D. V. Konarev, S. S. Khasanov, A. Otsuka, et al., Chem.-Eur. J. **9**, 3837 (2003). https://doi.org/10.1002/chem.200204470
29. D. V. Konarev, S. S. Khasanov, G. Saito, et al., *Proceedings of the International Young Scientist Workshop "Chemistry of Porphyrins and Related Compounds,"* Ivanovo, 2012 (Ivanovo, 2012), p. 59 [in Russian].
30. J. Kim, S. H. Lim, Y. Yoon, et al., Tetrahedron Lett. **52**, 2645 (2011). https://doi.org/10.1016/j.tetlet.2011.03.048
31. L. Zheng, Y. Dan, L. Xiong, et al., Anal. Chim. Acta **768**, 69 (2013). https://doi.org/10.1016/j.aca.2013.01.019
32. K. Deng, J. Zhou, and X. Li, Electrochim. Acta **114**, 341 (2013). https://doi.org/10.1016/j.electacta.2013.09.164
33. M. Prato, M. Maggini, C. Giacometti, et al., Tetrahedron **52**, 5221 (1996). https://doi.org/10.1016/0040-4020(96)00126-3
34. N. G. Bichan, E. N. Ovchenkova, M. S. Gruzdev, et al., Russ. J. Struct. Chem. **59**, 711 (2018). https://doi.org/10.1134/S0022476618030320
35. E. V. Motorina, T. N. Lomova, and M. V. Klyuev, Makrogeterotsikly **6**, 327 (2013). https://doi.org/10.6060/mhc130644l
36. N. G. Bichan, E. N. Ovchenkova, N. O. Kudryakova, et al., J. Coord. Chem. **70**, 2371 (2017). https://doi.org/10.1080/00958972.2017.1335867
37. A. Mansour, M. Zaied, I. Ali, et al., Polyhedron **127**, 496 (2017). https://doi.org/10.1016/j.poly.2016.10.031
38. J. Macka, M. J. Stillman, and N. Kobayashi, Coord. Chem. Rev. **251**, 429 (2007).
39. Y. Terazono, B. O. Patrick, and D. H. Dolphin, Inorg. Chim. Acta **346**, 265 (2003).
40. M. C. Martin, X. Du, and L. Mihaly, Phys. Rev. B **50**, 173 (1994).
41. E. N. Ovchenkova, N. G. Bichan, and T. N. Lomova, Russ. J. Org. Chem. **52**, 1503 (2016). https://doi.org/10.1134/S1070428016100213
42. N. G. Bichan, E. N. Ovchenkova, N. O. Kudryakova, et al., New J. Chem., No. 42, 12449 (2018). https://doi.org/10.1039/C8NJ00887F
43. F. D' Souza, G. R. Deviprasad, M. E. Zandler, et al., J. Phys. Chem. A **106**, 3243 (2002). https://doi.org/10.1021/jp013165i
44. F. D' Souza, G. R. Deviprasad, M. E. Zandler, et al., J. Phys. Chem. A **107**, 4801 (2003). https://doi.org/10.1021/jp030363w
45. P. A. Troshin, A. S. Peregudov, D. Muhlbacher, et al., Eur. J. Org. Chem., No. 14, 3064 (2005). https://doi.org/10.1002/ejoc.200500048
46. K. M. Kadish, X. Q. Lin, and B. C. Han, Inorg. Chem. **26**, 4161 (1987). https://doi.org/10.1021/ic00272a006

Translated by O. Fedorova